Construction Algorithm for Adaptive Morphological Structuring Elements Based on the Neighborhood Gray Difference Changing Vector Field and Relative Density

CHAO FANG, XIAO-PENG WANG, QING-SHENG WANG, AND JIN-CHENG LIANG

School of Electronic and Information Engineering, Lanzhou Jiaotong University, Lanzhou 730070, China

Corresponding author: Xiao-Peng Wang (wangxiaopeng@mail.lzjtu.cn)

ABSTRACT Structuring elements of fixed shape and size are used in most conventional mathematical morphology operations, which makes the border of image targets shift, produces new image artifacts and loses small image objects due to the diversity and complexity of the image targets. In this paper, a new construction algorithm for adaptive structuring elements is proposed based on the neighborhood gray difference changing vector field and relative density. The proposed structuring element is able to adaptively change shape according to the gray and edge characteristics of an image. This algorithm involves first incorporating the gray difference changing vector field to smooth the local image region and make the gray level within the image target more uniform and then defining a border degree function based on relative density to determine whether the center pixel of the local image region is a border pixel. The adaptive structuring element is composed of all the strong border pixels found in a local image region. Dilation and erosion operations and other derivative operations are proposed with this new adaptive structuring element based on conventional morphology operation principles. The experimental results show that this proposed algorithm is able to effectively suppress the shifting effect of the image target borders while accurately locating the border of the image target region. Additionally, other effective image information is retained and image distortion is reduced while weakening the image details.

INDEX TERMS Mathematical morphology, adaptive structuring element, gray difference changing vector field, relative density.

I. INTRODUCTION

Mathematical morphology [1], [2] is a theory based on set theory, integral geometry and grid algebra that is used to analyze the geometric structure characteristics of images and to extract image features using structuring elements of a certain shape and size to perform morphology operations on all the pixels. Image morphology operations are able to remove irrelevant image structures, simplify image data and extract nonlinear features. However, in real applications,

morphology operations with structuring elements of a fixed shape and size can easily change the features of image objects, such as image object border shifting, image artifact occurrences and small image object losses due to the complexity and variety of image contents and differences in the shape and size of image objects. For this reason, researchers have proposed a variety of adaptive structuring element construction methods, which can be roughly divided into the following three categories. The first category includes the methods where the shape of the structuring element changes with respect to the local characteristics of the image. Beucher *et al.* [3] presented a method where the adaptive

The associate editor coordinating the review of this manuscript and approving it for publication was Abdel-Hamid Soliman.

structuring elements can be used in traffic video processing to make the structuring element adaptively change shape with respect to changes along the vehicle vertical direction and then extract and label the vehicle. Lerallut *et al.* [4] presented a method that utilizes morphological amoeba to construct adaptive structuring elements. This method is achieved by weighted geodesic distances and local target contour features of the image. Álvar *et al.* [5] proposed a multidirectional vector field adaptive morphology filter based on local features of an image. This method constructs a multidirectional vector field mainly based on the direction of the contours in the image and adjusts the shape of the structuring element with the multidirectional vector field. Zhang and Wang [6] proposed an effective opening and closing morphological mean filter to remove impulse noise in digital images. During the noise detection phase, point-adapted structuring elements are constructed using the labeled image. This method can effectively remove high-density impulse noise while retaining the image details. The second category includes the methods where the size of the structuring element changes with respect to the local characteristics of the image. Shi *et al.* [7] proposed an adaptive edge detection algorithm for magnetic resonance imaging (MRI) based on morphology. This algorithm is achieved by adjusting the weights of structuring element detection results in each direction to construct structuring elements with variable sizes. Curic *et al.* [8] proposed a Salience adaptive structuring element construction method. The size of the structuring element can adaptively change according to the convex angle of the edge in the image, and the antinoise performance is better than that provided by morphological amoebae. Wang *et al.* [9] developed an adaptive structuring element construction method based on morphological gradients, which mainly decomposes morphological gradients into multiple levels based on gradient values, where low gradients use larger structuring elements while high gradients use smaller structuring elements. Lei *et al.* [10] employed multiscale structuring elements to reconstruct a gradient image. The third category includes the methods where the shape and size of structuring elements adaptively change with respect to the local characteristics of the image. Mallat and Youssef [11] proposed an adaptive structuring element construction method that uses an inertia tensor to estimate the local structural geometric characteristics where the closed operation of structuring elements can achieve the purpose of recovering distorted information. Li *et al.* [12] proposed a multidirectional and multiscale construction method of linear structuring elements, which can extract straight structures in images. Ti *et al.* [13] proposed a contour-guided adaptive morphological filtering method that can effectively recover depth images. Bai *et al.* [14] proposed a method for constructing adaptive structuring elements based on local features and pixel distances of color images where elements can better maintain the relevance of color images. Makhlouf and Daamouche [15] proposed an adaptive structuring element construction method suitable for road recognition in very high resolution (VHR) images. This method is achieved by combining road spectral characteristics and spatial characteristics to construct adaptive structuring elements. Pinoli and Debayle [16] proposed a method for constructing adaptive structuring elements that uses image brightness, contrast, curvature and other feature functions and tolerances to build adaptive neighborhoods. Das *et al.* [17] proposed a scheme for automatic generation of structuring elements based on common handwriting styles. Khurshid *et al.* [18] used the frequency information provided by the discrete wavelet transform (DWT) to assign adaptive structuring elements for each pixel in the image, where smaller structuring elements were assigned for pixels with higher frequency content and larger structuring elements were assigned for lower frequency pixels. Lei *et al.* [19] propose a conditionally invariant morphological framework based on the proposed vector ordering. Landström and Thurley [20] used the local structure tensor to define adaptive elliptical structuring elements.

In summary, the method of constructing adaptive structuring elements is mainly based on the local similarity characteristics or image edge characteristics of adjacent pixels in an image. Among all the structuring element construction methods above, the methods based on similar characteristics have better regional adaptability and less noise sensitivity, whereas the methods based on edge characteristics can maintain the geometrical characteristics of the image target to the greatest extent and reduce the distortion of structural details of the image target.

In this paper, a construction algorithm for adaptive morphology structuring elements is proposed based on neighborhood grayscale difference changing vector field and relative density. This algorithm uses the grayscale and border (edge pixels) characteristics of an image to construct adaptive morphology structuring elements with variable shapes. In the morphological operation, the adaptive structuring elements can correspond to the shape of the image target, thereby maintaining the integrity of the necessary information of the target, improving the accuracy of locating the border of the image target region, and reducing the distortion of the target structure details. This proposed algorithm is achieved by first smoothing the local region in the image using the neighborhood grayscale difference changing vector field and then determining whether the center pixel of a local region is a border pixel by using a border degree function based on relative density. The constructed adaptive structuring element is composed of all the strong border pixels.

This paper is organized as follows. Section II describes the basic mathematical morphology operations. Section III introduces the construction of the adaptive structuring element in two individual parts: (1) the image smoothing based on the neighborhood gray difference changing vector field and (2) the image border pixel detection based on relative density. Section IV introduces the morphology operations with the adaptive structuring elements. The experimental results are described in Section V. Finally, Section VI is the conclusion section, which presents the overall remarks on the achieved results.

II. BASIC MATHEMATICAL MORPHOLOGY OPERATIONS

Conventional mathematical morphology is a tool for mathematical analysis of images based on structuring elements. The role of structuring elements in morphology operations is equivalent to the filter window in signal processing. There are two basic morphology operations: erosion and dilation operations and opening and closing operations. Suppose that $f(x, y)$ is the original image and $b(m, n)$ is the structuring element. Then, $f_e(x, y)$, $f_d(x, y)$, $f_o(x, y)$ and $f_c(x, y)$ are the results of erosion, dilation, opening, and closing operations respectively. The erosion, dilation, opening, and closing operations on grayscale image are defined as follows:

$$f_e(x, y) = f(x, y) \ominus b(m, n)$$
$$= \min \{f(x + m, y + n) - b(m, n)\} \quad (1)$$

$$f_d(x, y) = f(x, y) \oplus b(m, n)$$
$$= \max \{f(x - m, y - n) + b(m, n)\} \quad (2)$$

$$f_o(x, y) = f(x, y) \circ b(m, n)$$
$$= [f(x, y) \ominus b(m, n)] \oplus b(m, n) \quad (3)$$

$$f_c(x, y) = f(x, y) \bullet b(m, n)$$
$$= [f(x, y) \oplus b(m, n)] \ominus b(m, n) \quad (4)$$

where $\ominus$ is the erosion operation, $\oplus$ is the dilation operation, $\circ$ is the opening operation and $\bullet$ is the closing operation. Structuring elements with fixed shape and size are commonly used in conventional mathematical morphology operations. However, it is not practical to adapt such structuring elements to the size and shape of the image target, since it leads to the loss or change of the target characterristic information, such as target border contour shifts, fake target production and small target losses, due to the complexity and diversity of the image targets. Therefore, constructing adaptive structuring elements with variable shapes and sizes based on attributes such as the local characteristics of the image is the key to maintaining the integrity of the information of the target in the image.

III. CONSTRUCTION OF THE ADAPTIVE STRUCTURING ELEMENT

The main step to construct the adaptive structuring element is to construct adaptive structuring elements with variable shapes according to the grayscale and border characteristics in the image. To achieve this aim, two 3×3 masks, *SE* and *M*, are first designed. The local region Q_{SE}, whose center pixel P_{SE} is the pixel $f(3, 3)$, covered by the mask *SE* is created, and all the pixels in Q_{SE} are regarded as the fundamental elements of structuring element construction. Then, each pixel in Q_{SE} is regarded as the center pixel P_M, and Q_M, whose center pixel is P_M, is covered by M. The local region Q_M is then smoothed by the adaptive threshold value obtained by the neighborhood gray difference changing vector field to ensure that the gray levels in the same target region are basically
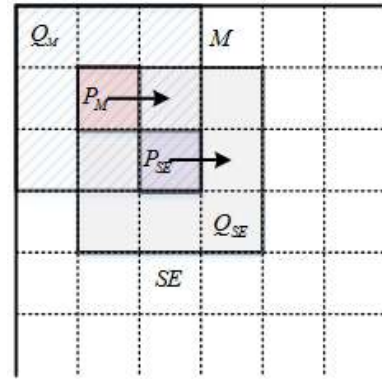

FIGURE 1. Construction of the adaptive structuring element.

consistent. Fig. 1 depicts the description given above. Next, whether the center pixel P_M in the local region Q_M is a border pixel is determined by a defined border degree function based on relative density. Finally, a structuring element composed of all the strong border pixels detected in the local region Q_{SE} is constructed. The mask *SE* is then shifted by a distance of a single pixel to obtain a new local region and another structuring element composed of all the strong border pixels in this region. The set containing all the structuring elements after traversing the image is the constructed adaptive structuring element.

In conclusion, there are two vital steps to construct the adaptive structuring element. First, smooth the local region covered by the mask *M* in the image by the neighborhood gray difference changing vector field. Second, define the border degree function based on the relative density to detect border pixels in the local region covered by the mask *SE*.

A. IMAGE SMOOTHING BASED ON THE NEIGHBORHOOD GRAY DIFFERENCE CHANGING VECTOR FIELD

In theory, grayscale, contrast, texture, and gradient characteristics are supposed to be similar in the same target region. However, the characteristics of the target region in the acquired image are not identical due to certain influences, including lighting and noise in the acquisition device. The accuracy of border pixel detection would be affected if the border pixel detection based on relative density is directly performed on the image. As a consequence, it is necessary to perform presmoothing on the image so that the gray levels of the target region tend to be consistent; accordingly, the accuracy of border pixel detection tends to be improved, and the actual position of the border pixels is finally detected. For this reason, an image smoothing method based on the neighborhood gray difference changing vector field is proposed. Based on the assumption that the gray level of the pixels within the target region should be similar to a certain extent, the gray level changes in all directions of the neighborhoods in the target and the changing vector of the orthogonal neighborhood gray
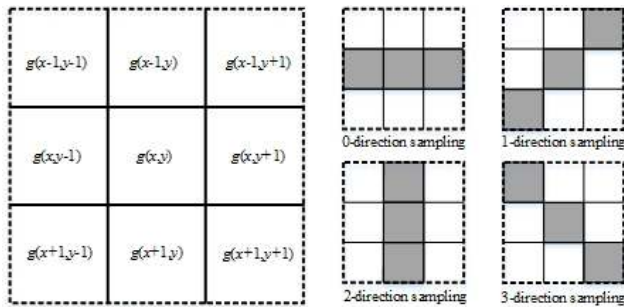
FIGURE 2. Approach to get the gray difference changing vector: (a) 3 × 3 neighborhood gray difference matrix and (b) neighborhood gray difference changing vector sampling template.

difference are both very small. As a result, the average value of the gray difference of the smaller orthogonal neighborhood gray difference changing vector can be selected as the threshold to smooth the image. The implementation process is as follows:

STEP 1: Compute the absolute gray level difference between a pixel and the center pixel in the 3 × 3 local region Q_M, denoted as $g(x \pm k, y \pm k)(k = 0, 1)$, to form a 3 × 3 neighborhood gray difference matrix.

STEP 2: As shown in Fig. 2, the sample gray levels in the obtained neighborhood gray difference matrix along 4 directions are used to get a gray difference changing vector, denoted as $a_i(i = 0, 1, 2, 3)$, which is calculated as follows:

$$\begin{cases} a_0 = g(x, y - 1) + g(x, y) + g(x, y + 1) \\ a_1 = g(x - 1, y + 1) + g(x, y) + g(x + 1, y - 1) \\ a_2 = g(x - 1, y) + g(x, y) + g(x + 1, y) \\ a_3 = g(x - 1, y - 1) + g(x, y) + g(x + 1, y + 1) \end{cases} \quad (5)$$

STEP 3: The mutually orthogonal neighborhood gray difference changing vector can be used as a basis for distinguishing the target border from the target. Inside the neighborhood in the target, the gray level changes in each direction and orthogonal neighborhood gray difference changing vector are both small. After the neighborhood gray difference changing vector is calculated, the orthogonal difference pair and minimum orthogonal difference are defined as follows:

$$\begin{cases} d_0 = a_0 - a_2 \\ d_1 = a_1 - a_3 \end{cases} \quad (6)$$

$$v = \min |d_0, d_1| \quad (7)$$

where d_0 and d_1 are the orthogonal difference along the 0, 2 directions and 1, 3 directions, respectively, and v is the minimum orthogonal difference.

STEP 4: Obtain the required threshold for image smoothing based on the minimum orthogonal difference v. The threshold adaptively changes according to v in each local region Q_M. If v equals d_0, the threshold τ is the quotient of the sum of the gray differences in all the neighborhoods in the 0 and 2 directions and the number of elements whose gray level differences in the neighborhoods along the 0 and 1

directions are not zero. If v equals d_1, the threshold τ is the quotient of the sum of the gray level differences in all the neighborhoods along the 1 and 3 directions and the number of elements whose gray level differences in the neighborhoods along the 1 and 3 directions are not zero. If $d_0 = d_1$, the threshold τ is the quotient of the sum of the gray level differences in all the neighborhoods along the 4 directions and the number of elements whose gray level differences in the neighborhoods along the 4 directions are not zero.

STEP 5: Smooth the local region using the obtained adaptive threshold by calculating the gray level difference between the pixel and the center pixel in the local region Q_M and by comparing the gray level differences with the threshold value τ. If the gray level difference is smaller than τ, then the corresponding pixel is regarded as similar to the center pixel and is replaced by the center pixel. Otherwise, the pixel is unchanged.

B. IMAGE BORDER PIXEL DETECTION BASED ON RELATIVE DENSITY

After smoothing, the gray levels of the pixels in the same target region in the image tend to be consistent and the separability between the border pixels and the pixels within the target is improved. The image can be divided into different regions according to different gray levels, and each pixel has a different density in different regions. The border pixels refer to the pixels located at the borders of different density regions, which indicates the structural information of the gray level distribution and different characteristics of pixels. According to whether the pixel is on the border, the pixels can be divided into border pixels and internal pixels. If the distribution of pixels in the neighborhood K (the gray value of pixels in K are the same as the gray value of the pixel p), whose center pixel is p, is concentrated on one side, as shown in Fig. 3 (a), then the pixel p is considered to be a border pixel. If the distribution is relatively uniform, then the pixel p is considered to be an internal pixel, as shown in Fig. 3 (b).
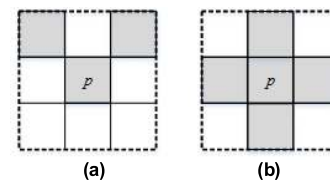

FIGURE 3. Distribution of a border pixel and an internal pixel: (a) p is a border pixel and (b) p is an internal pixel.

Based on the above principles, a border degree function based on the relative density can be used to determine whether the center pixel of a local region is a border pixel. In the K neighborhood of the pixel p, the density of the neighborhood K is defined as the number of pixels with the same gray value of pixel p (including pixel p) and is denoted as D_P. The relative density of the neighborhood K is defined as the quotient of the total number of the pixels in the neighborhood K and is denoted as D_{RP}. The distribution of a border pixel in the neighborhood K is sparser than the distribution of an

internal pixel; therefore, the D_P and D_{RP} of a border pixel are smaller than those of an internal pixel. For non-edge pixels, the gray level differences among the 8 nearest neighbors is small and the relative density is large. For edge pixels, the gray differences among the 8 nearest neighbors is large and the relative density is small due to the sharp change in the gray level. The judgment process of border pixels is as follows:

STEP 1: Reassign all the gray levels of the pixels within the smoothed local region Q_M; hence, assign the pixel gray levels that are equal to the gray value of the center pixel and the rest of the pixel gray levels to 1 and 0.

STEP 2: Define the border degree function.

To determine the degree of aggregation of the pixel density distribution in the 3×3 subregion Q_M, using the center pixel of Q_M as an anchor, create 2×2 masks consisting of the upper-left, upper-right, lower-left, and lower-right pixels and masks composed of 0, 2 direction and 1, 3 direction pixels, as shown in Fig. 4. Denote the masks as $S_i(i = 1, 2, 3, 4, 5, 6)$.
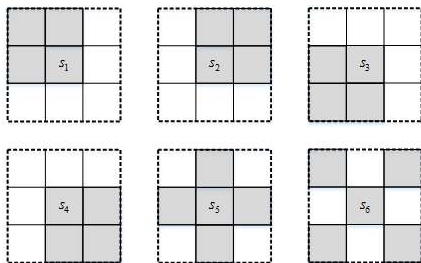

FIGURE 4. Constructed masks.

From a geometric point of view, border pixels are far away from some pixels with high-density gray levels and close to pixels with low-density gray levels and are located at the borders of different density regions. The density of the local region Q_M is defined as the number of pixels with a gray value of 1 in the 3×3 local region Q_M and is denoted as D_M. The density of $S_i(i = 1, 2, 3, 4, 5, 6)$ is defined as the number of pixels with a gray value of 1 in $S_i(i = 1, 2, 3, 4, 5, 6)$ and is denoted as $D_i(i = 1, 2, 3, 4, 5, 6)$. The border degree B, whose range is [0,1], is defined as the quotient of the maximum value in mask density $D_i(i = 1, 2, 3, 4)$ of the upper-left, upper-right, lower-left and lower-right 2×2 masks in Q_M and D_M. The larger the value of B is, the larger the density difference among the upper-left, upper-right, lower-left and lower-right regions, thereby leading to a higher possibility that the center pixel is located on the border among different regions.

When $D_M = 9$ or 8, the center pixel P_M in the local region Q_M is an internal pixel, as shown in Fig. 5.

When $D_M = 7$ and $\max(D_1, D_2, D_3, D_4) = 4$, since the local region Q_M is symmetric about the center, the distribution of the pixels in Q_M can be divided into the following six categories, as shown in Fig. 6 (a) through (f). The center pixels in Fig. 6 (a), (c), (d), and (e) are considered to be strong border pixels; hence, the border degree $B = \max(D_1, D_2, D_3, D_4)/D_M = 4/7$ and $D_5 \neq 5$;
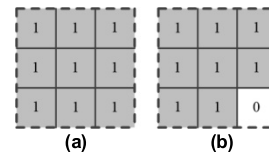

FIGURE 5. Distribution of pixels in the 8 neighborhoods: (a) $D_M = 9$ and (b) $D_M = 8$.
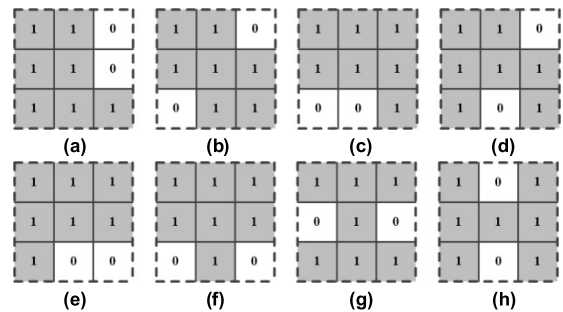

FIGURE 6. Distribution of pixels in the 8 neighborhoods ($D_M = 7$).

The center pixels in Fig. 6 (b) and (f) are considered to be strong internal pixels, so that the border degree $B = \max(D_1, D_2, D_3, D_4)/D_M = 4/7$ and $D_5 = 5$.

When $D_M = 7$ and $\max(D_1, D_2, D_3, D_4) = 3$, since the local region Q_M is symmetric about the center, the distribution of the pixels in Q_M can be divided into the following two categories, as shown in Fig. 6 (g) and (h). The center pixels in Fig. 6 (g) and (h) are considered to be weak border pixels; hence, the border degree $B = \max(D_1, D_2, D_3, D_4)/D_M = 3/7$ and $D_6 = 5$.

When $D_M = 7$, there is no case where the value of $\max(D_1, D_2, D_3, D_4)$ is less than 3.

The rest may be deduced by analogy, in which the process continues to analyze the values of B, D_5, and D_6 when the values of D_M are 6, 5, 4, 3, 2, and 1. Based on the taxonomic induction method, the border function is defined as shown in Eq. (8). This equation is able to determine whether the center pixel in the 3×3 local region Q_M is a border pixel.

$$
\begin{cases}
\text{Strong border pixels :} \\
\max(D_1, D_2, D_3, D_4) = 4 \& D_M \leq 7 \& \\
B = \max(D_1, D_2, D_3, D_4)/D_M \geq 4/7 \& D_5 \neq 5 \\
\max(D_1, D_2, D_3, D_4) = 3 \& D_M \leq 6 \& \\
B = \max(D_1, D_2, D_3, D_4)/D_M \geq 3/6 \& D_6 \neq 5 \\
\text{Weak border pixels :} \\
\max(D_1, D_2, D_3, D_4) = 3 \& D_6 = 5 \\
\max(D_1, D_2, D_3, D_4) < 3 \& D_M \leq 3 \\
\text{Internal pixel :} \\
\max(D_1, D_2, D_3, D_4) = 4 \& D_M \geq 5 \& D_5 = 5 \\
D_M > 7
\end{cases}
\tag{8}
$$

STEP 3: Detect border pixels.

Calculate the density D_M of the local region Q_M and the density $D_i(i = 1, 2, 3, 4, 5, 6)$ of the mask $S_i(i = 1, 2, 3, 4, 5, 6)$. Use the border degree function to determine

whether the center pixel of Q_M is a border pixel. Then, traverse M to acquire a new local region Q_M at a distance of a single pixel and determine whether the center pixel of Q_M is a border pixel until the determination of all the pixels in the local region Q_{SE} is completed. All the strong border pixels in the 3×3 local region Q_{SE} are regarded as the elements constituting the adaptive structuring element.

C. ADAPTIVE STRUCTURING ELEMENT CONSTRUCTION

The adaptive structuring element construction is mainly based on the border degree function defined by the local gray and edge feature changes of the image target, the neighborhood gray difference changing vector and the relative density. The implementation steps are as follows:

STEP 1: Design two 3×3 masks: SE and M.

STEP 2: Create a 3×3 local region Q_{SE} covered by SE in the original image with the pixel $f(3, 3)$ regarded as the. center pixel.

STEP 3: Create a 3×3 local region Q_M covered by M, where the first pixel in Q_{SE} is regarded as the center pixel of M.

STEP 4: Smooth Q_M by the neighborhood gray difference changing vector field method.

STEP 5: Determine whether the center pixel of Q_M is a border pixel by the border degree function based on relative density.

STEP 6: Traverse M at a distance of a single pixel to obtain a new 3×3 local region Q_M. Perform step 4 and step 5 until the determination of all pixels in Q_{SE} is completed. All the strong border pixels determined in Q_{SE} comprise the structuring element T_{SE}.

STEP 7: Traverse SE at a distance of a single pixel to obtain a new 3×3 local region Q_{SE}. Perform step 3 to step 6 until the determination of all the pixels in the original image is completed. The set containing all the structuring elements T_{SE} is the acquired adaptive structuring element.

IV. MORPHOLOGY OPERATIONS WITH THE ADAPTIVE STRUCTURING ELEMENT

After constructing the set containing the adaptive and variable structuring elements, the corresponding basic and adaptive morphology operations are able to be defined according to the conventional morphology operations. Similar to the conventional morphology operations, the adaptive morphology operations include adaptive dilation, erosion, opening and closing operations. Assume that $I(x, y)$ is the original image; $E(m, n)$ is the adaptive structuring element; $I_e(x, y)$, $I_d(x, y)$, $I_o(x, y)$ and $I_c(x, y)$ are the result images after the erosion, dilation, opening, and closing operations, respectively; and Θ, $\oplus$, $\circ$ and $\bullet$ are the erosion, dilation, opening, and closing operations, respectively. Then, the adaptive morphology

erosion, dilation, opening and closing operations are able to be defined as follows:

$$I_e(x, y) = I(x, y) \Theta E(m, n)$$
$$= \bigwedge_{(x,.y) \in E} I(x, y) \forall E \in I(x, y) \quad (9)$$

$$I_d(x, y) = I(x, y) \oplus E(m, n)$$
$$= \bigvee_{(x,.y) \in E} I(x, y) \forall E \in I(x, y) \quad (10)$$

$$I_o(x, y) = I(x, y) \circ E(m, n)$$
$$= [I(x, y) \Theta E(m, n)] \oplus E(m, n) \quad (11)$$

$$I_c(x, y) = I(x, y) \bullet E(m, n)$$
$$= [I(x, y) \oplus E(m, n)] \Theta E(m, n) \quad (12)$$

V. EXPERIMENTAL RESULTS AND ANALYSIS

To test the border preservation and antidistortion performance of the proposed adaptive structuring element in morphological operations, a simple binary image, a complex binary image and a grayscale image are used as experimental data. Experiments are performed using MATLAB R2017a with a 3.50 GHz/4G PC.

A. EXPERIMENTAL EVALUATION INDEXES

The Abdou-Pratt quality factor ($PFOM$), mean square error (MSE), peak signal-to-noise ratio ($PSNR$), structural similarity ($SSIM$), gradient magnitude similarity deviation ($GMSD$) and time complexity are used as numerical indexes in the border retention and image distortion experiments.

1) ABDOU-PRATT QUALITY FACTOR

The Abdou-Pratt quality factor $PFOM$ is defined as follows:

$$PFOM = \frac{1}{\max(N_e, N_d)} \sum_{k=1}^{N_d} \frac{1}{1 + ad^2(k)} \quad (13)$$

where N_e is the number of reference border pixels, N_d is the number of detected border pixels, $d(k)$ is the Euclidean distance between the first reference border pixel and the k_{th} detected border pixel, and a is a constant number equal to 1/9. In this paper, the artificial target border pixels are used as reference border pixels. The larger the $PFOM$ is, the higher the locating accuracy of the border pixels and the smaller the possibility of the detected border pixels shifting, which corresponds to better border retention.

2) MEAN SQUARE ERROR

The mean square value of the pixel difference between the original image and the processed image is calculated, and the magnitude of the mean square error is used to evaluate the distortion of the processed image. The mean square error MSE is defined as follows:

$$MSE = \frac{1}{MN} \sum_{i=1}^{M} \sum_{j=1}^{N} (f_1(i, j) - f_2(i, j))^2 \quad (14)$$

where M and N are the image sizes, $f_1(i,j)$ is the original image and $f_2(i,j)$ is the processed image.

3) PEAK SIGNAL-TO-NOISE RATIO

Peak signal-to-noise ratio $PSNR$ is defined as follows:

$$PSNR = 10 \log \frac{255 \times 255}{MSE} \qquad (15)$$

The peak signal-to-noise ratio is also a parameter used to measure the degree of image distortion. The larger the peak signal-to-noise ratio is, the lower the image distortion.

4) STRUCTURAL SIMILARITY

Structural similarity is a hypothesis based on the adaptive extraction of visual information by the human eye. Structural similarity $SSIM$ is defined as follows:

$$SSIM = \frac{(2\mu_1\mu_2 + C_1)}{(\mu_1^2 + \mu_2^2 + C_1)} \cdot \frac{(2\sigma_{12} + C_2)}{(\sigma_1^2 + \sigma_2^2 + C_2)} \qquad (16)$$

where μ_1 and μ_2 are the mean gray levels of the original image and the processed image, respectively; σ_1 and σ_2 are the variance of the original image and processed image, respectively; σ_{12} is the covariance between the original image and processed image; and C_1 and C_2 are constant numbers, which are equal to 6.5 and 8.5, respectively. The larger the $SSIM$ is, the lower the distortion of the processed image.

5) GRADIENT MAGNITUDE SIMILARITY DEVIATION

The gradient magnitude mainly indicates the image structure. When the image is distorted, the gradient magnitude is degraded to a certain extent. The similarity deviation of the gradient magnitude indicates the extent of distortion of the image. The gradient magnitude similarity deviation $GMSD$ is defined as follows:

$$m_r(i) = \sqrt{(f_1 \otimes h_x)^2 + (f_1 \otimes h_y)^2} \qquad (17)$$

$$m_d(i) = \sqrt{(f_2 \otimes h_x)^2 + (f_2 \otimes h_y)^2} \qquad (18)$$

where f_1 is the original image; f_2 is the processed image; h_x and h_y are linear filters along the horizontal and vertical directions, respectively; $m_r(i)$ and $m_d(i)$ are the gradient magnitudes of pixel i in image f_1 and f_2, respectively.

$$GMS(i) = \frac{2m_r(i)m_d(i) + c}{m_r^2(i) + m_d^2(i) + c} \qquad (19)$$

GMS is the similarity of the gradient magnitude, where c is a constant number equal to 200.

$$GMSM = \frac{1}{L} \sum_{i=1}^{L} GMS(i) \qquad (20)$$

$GMSM$ is the average gradient magnitude, where L is the number of image pixels.

$$GMSD = \sqrt{\frac{1}{N} \sum_{i=1}^{N} (GMS(i) - GMSM)^2} \qquad (21)$$

$GMSD$ is the deviation in the gradient magnitude similarity and indicates the distortion of the image. The larger the $GMSD$ value is, the more degraded the image.

B. EXPERIMENTAL RESULTS AND ANALYSIS ON BINARY IMAGES

To compare the image distortion and the image border retention of binary images caused by the morphological operations with the proposed adaptive structuring element and the conventional structuring elements, a simple binary image (350×280 pixels) and a complex binary image (500×459 pixels) are tested. Cross-shaped (5×5 size), circular (5×5 size), and adaptive structuring elements are used to perform erosion, dilation, and morphological difference operations on the images.

There are three image targets, a triangle, a circle and a square, in Fig. 7 (a). The differences in the results of the erosion operation on Fig. 7 (a) using the three structuring elements are not significant and the triangle in the image is sharper. The cross-shaped and the circular structuring elements are used to perform the dilation operation and the structural characteristics of the square and triangle in the image are changed. Cross-shaped depressions appear in the image targets in Fig. 7 (e), whereas the image targets in Fig. 7 (f) are smoother.

The results show that the morphological operations with the structuring elements that are dissimilar to the image target structure leads to a change in the original image target structures. After the dilation operation with the adaptive structuring element, the triangle in Fig. 7 (a) is smoothed, whereas the shape of the other objects are well retained. The proposed adaptive structuring element is composed of the image border characteristics and is similar to the geometric structure of the image target, so that it is able to well retain the geometric characteristics of the image target.

The image target (butterfly) in Fig. 8 (a) is complex, in which regular and irregular geometric structures coexist. Compared with the result of the adaptive structuring element, the details of the butterfly wing texture and antennae edges in the image are reduced (increased) to a greater extent by the erosion operation (dilation operation) with the cross-shaped and circular structuring elements. Morphology operations with structuring elements of fixed shape and size leads to the distortion of the image geometric structure, because the such elements cover a local region that is larger than the image border. The proposed adaptive structuring element is able to change its shape and size adaptively according to the local details of the image, which allows this element to retain the image geometric structure.

The numerical results of the dilation and erosion operations with different structuring elements on simple (Fig. 7 (a)) and complex binary images (Fig. 8 (a)) are shown in Tables 1 and 2, respectively. Among the three elements, the proposed adaptive structuring element has the smallest MSE and GMSD and the largest PSNR and SSIM in the dilation results. The proposed adaptive structuring element
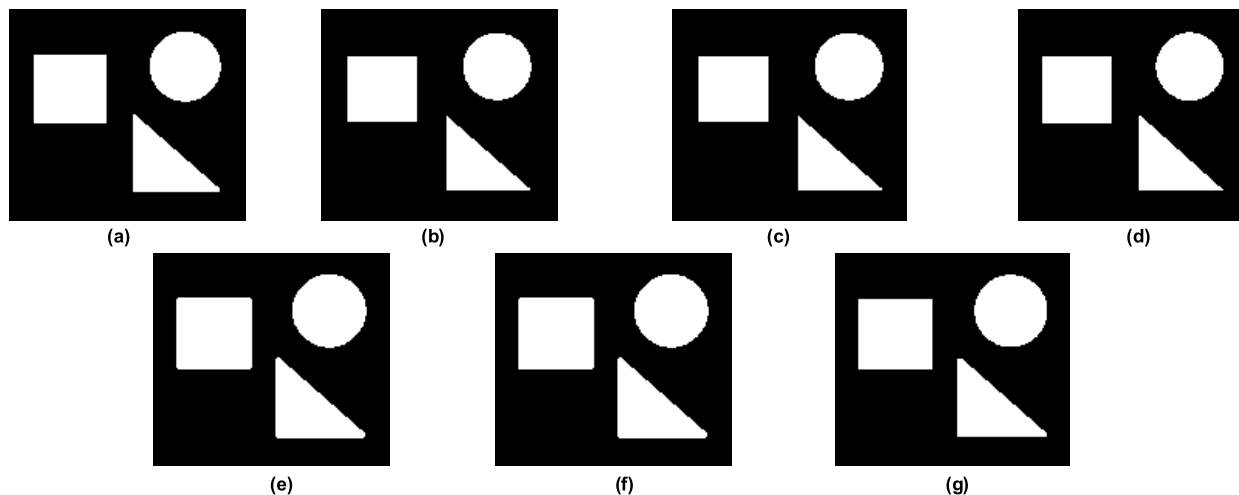
FIGURE 7. Results of erosion and dilation operations with different structuring elements on simple binary image. (a) Original image. (b) Result of erosion operation with cross-shaped structuring element. (c) Result of erosion operation with circular structuring element. (d) Result of erosion operation with proposed adaptive structuring element. (e) Result of dilation operation with cross-shaped structuring element. (f) Result of dilation operation with circular structuring element. (g) Result of dilation operation with proposed adaptive structuring element.

FIGURE 8. Results of erosion and dilation operations with different structuring elements on complex binary image. (a) Original image. (b) Result of erosion operation with cross-shaped structuring element. (c) Result of erosion operation with circular structuring element. (d) Result of erosion operation with proposed adaptive structuring element. (e) Result of dilation operation with cross-shaped structuring element. (f) Result of dilation operation with circular structuring element. (g) Result of dilation operation with proposed adaptive structuring element.
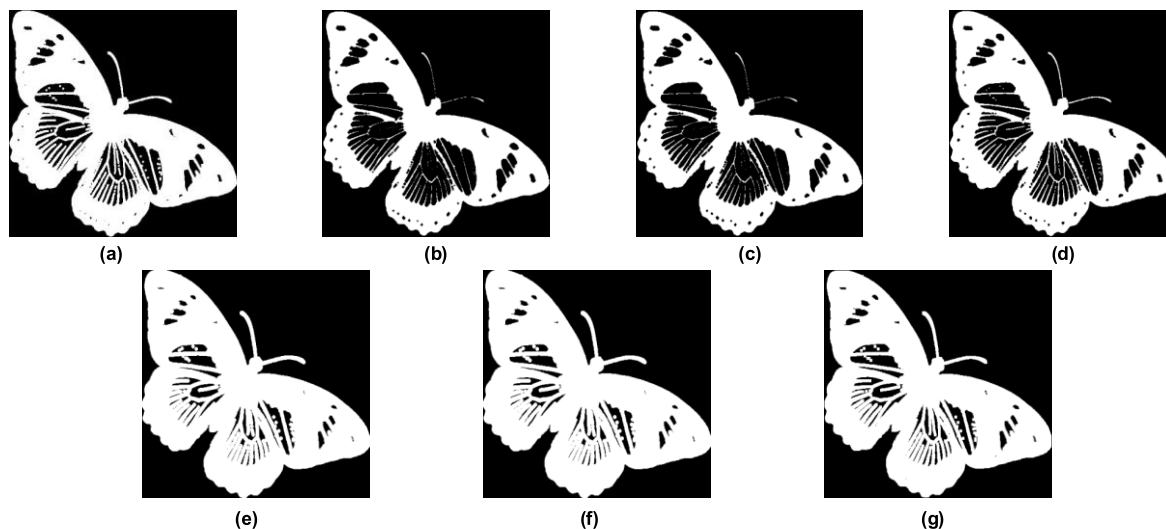
TABLE 1. Numerical results of the erosion and dilation operations with different structuring elements on a simple binary image.

Structuring elements	MSE		PSNR		SSIM		GMSD	
	Erosion	Dilation	Erosion	Dilation	Erosion	Dilation	Erosion	Dilation
Cross-shaped	0.0191	0.0196	65.3154	65.2055	0.9988	0.9988	8.0151×10^{-4}	8.0630×10^{-4}
Circular	0.0191	0.0197	65.3154	65.1920	0.9988	0.9988	6.8185×10^{-4}	6.8759×10^{-4}
Proposed adaptive	0.0118	0.0120	67.4285	67.3390	0.9994	0.9994	2.3896×10^{-4}	2.3902×10^{-4}

adaptively adjusts its shape according to the local border features of the image, which makes its shape structure similar to that of the image target, causing the lowest distortion of the target geometry among the structuring elements. The results show that the image distortion caused by the erosion and dilation operations with the proposed adaptive structuring elements is lower than that caused by the same operations with the other two structuring elements.

TABLE 2. Numerical results of the erosion and dilation operations with different structuring elements on a complex binary image.

Structuring elements	MSE		PSNR		SSIM		GMSD	
	Erosion	Dilation	Erosion	Dilation	Erosion	Dilation	Erosion	Dilation
Cross-shaped	0.0690	0.0627	59.7414	60.1613	0.9953	0.9960	7.5979×10^{-4}	7.8488×10^{-4}
Circular	0.0710	0.0638	59.6181	60.0850	0.9951	0.9959	7.7872×10^{-4}	8.0306×10^{-4}
Proposed adaptive	0.0483	0.0445	61.2917	61.6509	0.9978	0.9977	3.6768×10^{-4}	4.1516×10^{-4}

(a)   (b)   (c)   (d)

FIGURE 9. Results of border extraction by morphology difference operations with different structuring elements on simple binary image. (a) Borders extracted manually. (b) Result of morphological border extraction with cross-shaped structuring element. (c) Result of morphological border extraction with circular structuring element. (d) Result of morphological border extraction with proposed adaptive structuring element.

(a)   (b)   (c)

FIGURE 10. Results of border extraction by morphology difference operations with different structuring elements on local region in simple binary image. (a) Result of morphological border extraction with cross-shaped structuring element. (b) Result of morphological border extraction with circular structuring element. (c) Result of morphological border extraction with proposed adaptive structuring element.
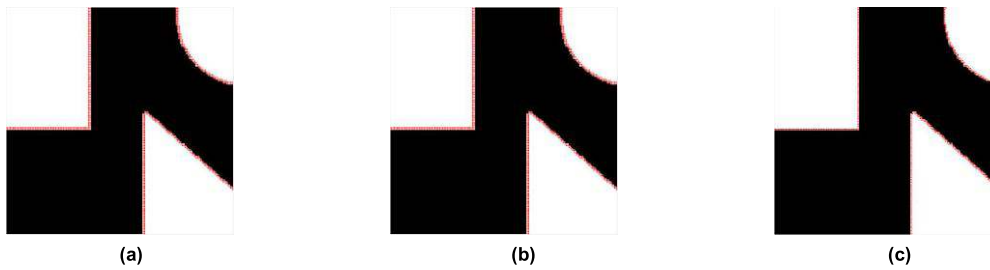

(a)   (b)   (c)   (d)

FIGURE 11. Results of border extraction by morphology difference operations with different structuring elements on complex binary image. (a) Borders extracted manually. (b) Result of morphological border extraction with cross-shaped structuring element. (c) Result of morphological border extraction with circular structuring element. (d) Result of morphological border extraction with proposed adaptive structuring element.

The results of the morphological difference operation on Fig. 7 (a) and Fig. 8 (a) using the three structuring elements are shown in Figs. 9 and 11, respectively. The results show that the edges extracted by the adaptive structuring elements and by hand are the most similar. To determine whether the image target border and the border pixels extracted by the morphological difference operation with the three structuring elements are shifted and missing, the border extraction results of the local regions in Fig. 7 (a) and Fig. 8 (a) are compared and analyzed in Fig. 10 and Fig. 12, respectively.

TABLE 3. Abdou-Pratt quality factors of morphology border extraction with different structuring elements on a simple binary image.

Structural elements	Cross-shaped	Circular	Proposed adaptive
Quality factor	0.6147	0.6147	0.9794

The results show that the morphological difference operation with the proposed adaptive structuring element does not produce the shifted target border and has better border
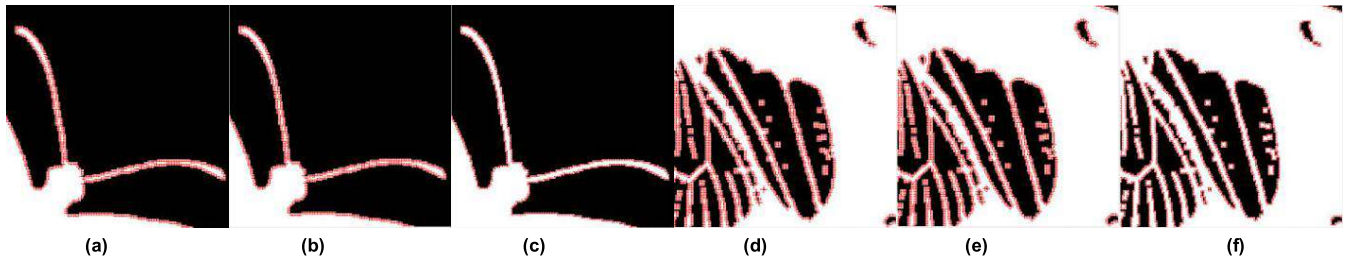
FIGURE 12. Results of border extraction by morphology difference operations with different structuring elements on local region in complex binary image. (a)&(d) Result of morphological border extraction with cross-shaped structuring element. (b)&(e) Result of morphological border extraction with circular structuring element. (c)&(f) Result of morphological border extraction with proposed adaptive structuring element.

FIGURE 13. Results of opening and closing operations with different structuring elements on grayscale image. (a) Original image. (b) Result of opening operation with cross-shaped structuring element. (c) Result of opening operation with circular structuring element. (d) Result of opening operation with Pinoli's [16] adaptive structuring element. (e) Result of opening operation with Landström's [20] adaptive structuring element. (f)Result of opening operation with proposed adaptive structuring element. (g) Result of closing operation with cross-shaped structuring element. (h) Result of closing operation with circular structuring element. (i) Result of closing operation with Pinoli's [16] adaptive structuring element. (j) Result of closing operation with Landström's [20] adaptive structuring element. (k) Result of closing operation with proposed adaptive structuring element.

TABLE 4. Abdou-Pratt quality factors of morphology border extraction with different structuring elements on a complex binary image.

Structural elements	Cross-shaped	Circular	Proposed adaptive
Quality factor	0.6967	0.6797	0.9695

TABLE 5. Time complexity of morphology difference operations with different structuring elements on a complex binary image.

Structural elements	Cross-shaped	Circular	Proposed adaptive
Erosion	0.081s	0.094s	3.519s
Dilation	0.097s	0.099s	3.698s

retention capabilities than the corresponding operations with the other elements. The image target borders produced by the morphological difference operation with the cross-shaped and circular structuring elements are both shifted inward.

The Abdou-Pratt quality factor results of the morphological difference operation with different structuring elements on simple and complex binary images are shown in Tables 3 and 4. The Abdou-Pratt quality factor of the

TABLE 6. Numerical results of erosion and dilation operations with different structural elements on 'Lena' image.

Structuring elements	MSE		PSNR		SSIM		GMSD	
	Opening	Closing	Opening	Closing	Opening	Closing	Opening	Closing
Cross-shaped	0.0413	0.0381	61.9723	62.3232	0.9975	0.9979	0.1025	0.0760
Circular	0.0462	0.0452	61.4812	61.5798	0.9971	0.9972	0.1051	0.0754
Pinoli's [16] adaptive	0.0111	0.0075	67.6922	69.4025	0.9995	0.9997	0.0783	0.1008
Landström's [21] daptive	0.0302	0.0262	63.3377	63.9479	0.9985	0.9988	0.0639	0.0372
Proposed adaptive	0.0265	0.0226	63.9051	64.5901	0.9989	0.9991	0.0704	0.0619

TABLE 7. Time complexity of the morphology difference operations with different structuring elements on the 'Lena' image.

Structuring elements	Cross-shaped	Circular	Pinoli's [16] adaptive	Landström's [20] daptive	Proposed adaptive
Erosion	0.388s	0.256s	4.855s	0.755s	2.271s
Dilation	0.221s	0.239s	4.833s	0.773s	2.308s

proposed adaptive structuring elements is the highest, indicating that this element has good boundary locating ability and boundary detail retaining ability.

The time complexity results of the morphological difference operation with different structuring elements on complex binary images are shown in Table 5. The time complexity of the proposed adaptive structuring elements is the highest, because the construction of the adaptive structuring element includes two processes: smoothing the local region and detecting border pixels. Therefore, the computation of the proposed adaptive structuring elements is relatively larger than that of the other elements.

C. EXPERIMENTAL RESULTS AND ANALYSIS ON GRAYSCALE IMAGES

To test the distortion of the image caused by the morphological operation with the proposed adaptive structuring element on a grayscale image, a grayscale image (256×256 pixels) named 'Lena' is utilized. The experimental results from opening and closing operations with 5×5 cross-shaped, 5×5 circular, Pinoli's [16], Landström's [20] and the proposed adaptive structuring elements are analyzed.

In Fig. 13, the light (dark) details of the hat, feathers, eyes, lips and other image targets are weakened by the opening (closing) operation with cross-shaped and circular structuring elements. Moreover, the details of the face, hat, and feather regions in the image are lost, which reduces the sharpness of the image. Although the light (dark) details of the hat, feathers, eyes, lips and other image targets are weakened by the opening (closing) operation with Pinoli's [16], Landström's [20] and the proposed adaptive structuring elements, the details of the features (texture features of the hat and feathers) in the image are preserved to a great extent. Additionally, the sharpness of the acquired image is higher than that in the images produced by the other two structuring elements. Furthermore, compared with the proposed adaptive structuring elements, Pinoli's [16] adaptive structuring elements have weaker capability to eliminate bright details (dark details) and stronger capability to retain image details. Compared

with the proposed adaptive structuring elements, Landström's [20] adaptive structuring elements have the same capability to eliminate bright details (dark details) and weaker capability to retain image details.

Among the three structuring elements (cross-shaped, circular and proposed adaptive structuring element), the proposed adaptive structuring element has the lowest MES and GMSD and the highest PSNR and SSIM in Table 6. These results indicate that the distortion of the image caused by the opening and closing operations with the proposed adaptive structuring element is less than that caused by the opening and closing operations with the other two structuring elements. The MES of the proposed adaptive structuring element is higher than that of Pinoli's [16] adaptive structuring element and lower than that of Landström's [20] adaptive structuring element. The GMSD of the proposed adaptive structuring element is higher than that of Landström's [20] adaptive structuring element and lower than that of Pinoli's [16] adaptive structuring element. The PSNR and SSIM of the proposed adaptive structuring element are higher than those of Landström's [20] adaptive structuring element and lower than those of Pinoli's [16] adaptive structuring element. These results imply that the distortion of the image caused by the opening and closing operations with the proposed adaptive structuring element is between that caused by the opening and closing operations with Pinoli's [16] and Landström's [20] adaptive structuring elements.

The time complexity results of the morphological difference operation with different structuring elements on the 'Lena' image is shown in Table 7. The time complexity of the three adaptive structuring elements is the higher than that of the cross-shaped and circular structuring elements. The time complexity of the proposed adaptive structuring element is between that of Pinoli's [16] and Landström's [20] adaptive structuring elements.

VI. CONCLUSION

In this paper, a morphological adaptive structuring element construction algorithm based on the neighborhood gray

difference change vector field and relative density is proposed. This algorithm is achieved by first smoothing the image by the neighborhood gray difference changing vector field that distinguishes the internal and external characteristics of the image targets, then defining a border degree function based on relative density to determine whether a pixel in the image is a border point, and finally by constructing a set containing adaptive structuring elements according to the local border characteristics of the image. The experimental results show that, compared with conventional structuring elements with fixed size and shape, morph ological operations and morphological difference operations with the adaptive structuring element are able to well preserve the border information and accurately locate the border of the image. Additionally, the loss of other details in the image is minimized while weakening the image details, thereby leading to lower distortion of the image.

REFERENCES

[1] G. Matheron, *Random Sets and Integral Geometry*. Hoboken, NJ, USA: Wiley, 1975.

[2] J. Serra, *Image Analysis and Mathematical Morphology*. London, U.K.: Academic, 1982, pp. 424–471.

[3] S. Beucher, J. Blosseville, and F. Lenoir, "Traffic spatial measurements using video image processing," *Proc. SPIE*, vol. 848, pp. 648–655, Feb. 1988.

[4] R. Lerallut, É. Decencière, and F. Meyer, "Image filtering using morphological amoebas," *Image Vis. Comput.*, vol. 25, no. 4, pp. 395–404, Apr. 2007.

[5] Á.-G. Legaz-Aparicio, R. Verdu-Monedero, and J. Angulo, "Adaptive morphological filters based on a multiple orientation vector field dependent on image local features," *J. Comput. Appl. Math.*, vol. 330, pp. 965–981, Mar. 2018.

[6] C. Zhang and K. Wang, "Removal of high-density impulse noise based on switching morphology-mean filter," *AEU-Int. J. Electron. Commun.*, vol. 69, no. 1, pp. 226–235, Jan. 2015.

[7] S. Wen, Z. Xuefang, and Z. Guang, "A daptive edge detection algorithm of MRI image based on morphology," *Chin. J. Sci. Instrum.*, vol. 34, pp. 408–413, Feb. 2013.

[8] V. Curic, C. L. L. Hendriks, and G. Borgefors, "Salience adaptive structuring elements," *IEEE J. Sel. Topics Signal Process.*, vol. 6, no. 7, pp. 809–819, Nov. 2012.

[9] X.-P. Wang, J. Li, and Y. Liu, "Watershed segmentation based on gradient relief modification using variant structuring element," *Optoelectron. Lett.*, vol. 10, no. 2, pp. 152–156, Mar. 2014.

[10] T. Lei, X. Jia, T. Liu, S. Liu, H. Meng, and A. K. Nandi, "Adaptive morphological reconstruction for seeded image segmentation," *IEEE Trans. Image Process.*, vol. 28, no. 11, pp. 5510–5523, Nov. 2019.

[11] K. Mallat and R. Youssef, "Adaptive morphological closing based on inertia tensor for structuring element estimation," in *Proc. Int. Symp. Signal, Image, Video Commun. (ISIVC)*, Tunis, Tunisia, 2016, pp. 253–258.

[12] L. Ding, A. Kuriyan, R. Ramchandran, and G. Sharma, "Multi-scale morphological analysis for retinal vessel detection in wide-field fluorescein angiography," in *Proc. IEEE Western New York Image Signal Process. Workshop (WNYISPW)*, Nov. 2017, pp. 1–5.

[13] C. Ti, G. Xu, Y. Guan, and Y. Teng, "Depth recovery for kinect sensor using contour-guided adaptive morphology filter," *IEEE Sensors J.*, vol. 17, no. 14, pp. 4534–4543, Jul. 2017.

[14] R. Bai, J. Wang, G. Liang, and Y. Li, "A new color adaptive mathematical morphology operator based on distance and threshold," in *Proc. 11th IEEE Int. Conf. Anti-Counterfeiting, Secur., Identificat. (ASID)*, Oct. 2017, pp. 69–73.

[15] Y. Makhlouf and A. Daamouche, "Automatic generation of adaptive structuring elements for road identification in VHR images," *Expert Syst. Appl.*, vol. 119, pp. 342–349, Apr. 2019.

[16] J.-C. Pinoli and J. Debayle, "General adaptive neighborhood mathematical morphology," in *Proc. 16th IEEE Int. Conf. Image Process. (ICIP)*, Cairo, Egypt, Nov. 2009, pp. 2249–2252.

[17] P. Das, T. Dasgupta, and S. Bhattacharya, "A novel scheme for bengali handwriting recognition based on morphological operations with adaptive auto-generated structuring elements," in *Proc. 2nd Int. Conf. Control, Instrum., Energy Commun. (CIEC)*, Kolkata, India, Jan. 2016, pp. 211–215.

[18] H. Khurshid, M. F. Khan, and A. Ahmed, "Supervised building extraction using morphological profiles with adaptive structures," in *Proc. AMS Conf.*, Kuala Lumpur, Malaysia, 2015, pp. 96–100.

[19] T. Lei, Y. Zhang, Y. Wang, S. Liu, and Z. Guo, "A conditionally invariant mathematical morphological framework for color images," *Inf. Sci.*, vol. 387, pp. 34–52, May 2017.

[20] A. Landström and M. J. Thurley, "Adaptive morphology using tensor-based elliptical structuring elements," *Pattern Recognit. Lett.*, vol. 34, no. 12, pp. 1416–1422, Sep. 2013.

CHAO FANG is currently pursuing the Ph.D. degree in rail transit communication engineering with the School of Electronic and Information Engineering, Lanzhou Jiaotong University.

He is currently a Lecturer with the School of Electronic and Information Engineering, Lanzhou Jiaotong University. His research interest includes image processing.

XIAO-PENG WANG received the Ph.D. degree from Northwestern Polytechnical University, Xi'an, China, in 2005.

He is currently a Professor and a Doctoral Supervisor with the School of Electronic and Information Engineering, Lanzhou Jiaotong University. His research interest includes image processing and analysis.

QING-SHENG WANG is currently pursuing the master's degree with the School of Electronic and Information Engineering, Lanzhou Jiaotong University. His research interest includes image processing.

JIN-CHENG LIANG is currently pursuing the master's degree with the School of Electronic and Information Engineering, Lanzhou Jiaotong University. His research interest includes image processing.

• • •